



ELSEVIER

J. Non-Newtonian Fluid Mech. 100 (2001) 127–149

**Journal of
Non-Newtonian
Fluid
Mechanics**

www.elsevier.com/locate/jnnfm

Nonlinear stability of Poiseuille flow of a Bingham fluid: theoretical results and comparison with phenomenological criteria

C. Nouar^a, I.A. Frigaard^{b,*}

^a LEMTA, CNRS UMR 7563, UHP & INPL, 2 Avenue de la forêt de Haye, BP 160, 54504 Vandoeuvre, France

^b Department of Mathematics and Department of Mechanical Engineering, University of British Columbia,
2324 Main Mall, Vancouver, BC, Canada V6T 1Z4

Received 8 February 2001; received in revised form 16 July 2001

Abstract

We present new results on the nonlinear stability of Bingham fluid Poiseuille flows in pipes and plane channels. These results show that the critical Reynolds number for transition, Re_c , increases with Bingham number, B , at least as fast as $Re_c \sim B^{1/2}$ as $B \rightarrow \infty$. Estimates for the rate of increase are also provided. We compare these bounds and existing linear stability bounds with predictions from a series of phenomenological criteria for transition, as $B \rightarrow \infty$, concluding that only Hanks [AIChE J. 9 (1963) 306; 15 (1) (1963) 25] criteria can possibly be compatible with the theoretical criteria as $B \rightarrow \infty$. In the more practical range of application, $0 \leq B \leq 50$, we show that there exists a large disparity between the different phenomenological criteria that have been proposed. © 2001 Elsevier Science B.V. All rights reserved.

Keywords: Bingham fluid; Nonlinear stability; Phenomenological criteria

1. Introduction

Parallel duct flows of slurries and suspensions are relatively common in the petroleum and mining industries, where prediction of the flow regime can be an important design parameter in hydraulic systems. These complex fluids are commonly visco-plastic, meaning that they are characterised rheologically by having a yield stress, below which no deformation takes place. Our focus is on the simplest model for an inelastic yield stress fluid, namely a Bingham fluid. Although widely accepted that a Bingham fluid Poiseuille flow will be *more stable* than the same flow of a Newtonian fluid (i.e. with a viscosity equal to

* Corresponding author. Fax: +1-604-822-6074.

E-mail address: frigaard@math.ubc.ca (I.A. Frigaard).

the plastic viscosity of the Bingham fluid), there is no rigorous theoretical argument that establishes this fact. Such an argument is provided here.

We consider the nonlinear stability of a Poiseuille flow, between parallel plates and in a circular pipe. The fully established laminar velocity profile has a central *plug* region where the shear stress is less than the yield stress, the size of which depends only on the Bingham number of the flow, B . Our study is therefore focused at determining the effect of B on stability of the fully developed laminar flow. We derive new theoretical results and compare these with existing predictions. Existing studies of the stability of these flows can be separated into two broad classes: theoretical and phenomenological.

Theoretical studies of the stability of these flows are uncommon. The main difficulty is to deal with the unyielded plug region. The classical approach adopted for Newtonian (and many non-Newtonian) fluid Poiseuille flows has been to consider linear stability first, via the Orr–Sommerfeld equations, and then develop weakly nonlinear theories based on the linear theory. The linear theory can be developed for a Bingham fluid, with the proviso that the unyielded plug region is only linearly perturbed and does not break up. The plane channel problem has been analysed in [1]; there is no known analysis of the pipe flow problem. Since Hagen–Poiseuille flow of a Newtonian fluid is believed to be linearly stable (see [2–5]), study of the Bingham fluid problem is likely to be non-productive.

To extend these studies in the classical way to weakly nonlinear perturbations of a Bingham fluid has failed. For a nonlinear perturbation, we can no longer assume that unyielded fluid is contained in a single plug region and the classical description of the (possibly infinite) yield surface positions therefore becomes impractical. Instead, methods based on weak formulations (i.e. variational and energy stability methods), which ignore the positions of the yield surfaces, come to the fore. Energy stability methods for Newtonian fluid Poiseuille flows in channels, pipes and annuli were developed in the late 1960s [6,7], and are explained fully in [8]. We adapt these methods here to Bingham fluid flows. An advantage of these methods is that, through functional analytic arguments, completely rigorous lower bounds for stability can be produced. The disadvantage is that for many flows, including Poiseuille flows, the stability bounds are quite conservative, e.g. Busse [6] predicts a lower bound of $Re_c \geq 99.207$ for plane Poiseuille flow and Joseph and Carmi [7] predict $Re_c \geq 81.49$ for Hagen–Poiseuille flow. Experimentally obtained values for transition are an order of magnitude higher in both cases.

Phenomenological stability theories began to appear in the literature in the 1950s and are widely used in industrial applications. A general approach is to form a parametric ratio of various physical flow quantities that are supposed to determine the stability of the flow. The value of this parametric ratio at which the Newtonian flow becomes unstable is known or calculated. It is then assumed that the same value of this parametric ratio will govern stability for analogous flows of all purely viscous non-Newtonian fluids. There are numerous examples of such criteria, which we summarise in Section 4.

An outline of the paper is as follows. After a brief introduction in Section 2, we present our new results on the nonlinear stability of Poiseuille flows of a Bingham fluid (see Section 3). These results provide lower bounds for the critical Reynolds number needed for transition and the lower bounds vary with Bingham number B . In Section 4, we summarise the many phenomenological criteria that exist, that also predict transition for varying B . For the plane channel, the linear stability bounds in [1] provide a theoretical upper bound on the Reynolds number needed for transition. In Section 5, we provide a comprehensive comparison of our theoretical upper and lower bounds for transition with the different phenomenological criteria. We concentrate in particular on the behaviour for large B . The paper concludes with a discussion, in which we point out some interesting problems for continued research.

2. Bingham–Poiseuille flows

We investigate the stability of both plane and Hagen–Poiseuille flows of a single Bingham fluid. As far as is possible, we treat the two geometries together. Our flows satisfy the following dimensionless equations of motion:

$$\left[\frac{\partial u_i}{\partial t} + u_j \frac{\partial u_i}{\partial x_j} \right] = -\frac{\partial p}{\partial x_i} + \frac{1}{Re} \frac{\partial}{\partial x_j} \tau_{ij}, \quad (1)$$

$$\frac{\partial u_j}{\partial x_j} = 0, \quad (2)$$

where $p(\mathbf{x}, t)$ denotes the modified pressure (i.e. incorporating the static pressure gradient), $\mathbf{u}(\mathbf{x}, t)$ is the velocity and $\tau_{ij}(\mathbf{x}, t)$ the deviatoric stress. Boundary conditions of no-slip at the walls of the duct are imposed. The scaled constitutive laws are

$$\dot{\gamma}(\mathbf{u}) = 0 \Leftrightarrow \tau(\mathbf{u}) \leq B, \quad (3)$$

$$\tau_{ij}(\mathbf{u}) = \left[1 + \frac{B}{\dot{\gamma}(\mathbf{u})} \right] \dot{\gamma}_{ij}(\mathbf{u}) \Leftrightarrow \tau(\mathbf{u}) > B, \quad (4)$$

where the rate of strain and deviatoric stress second invariants, $\dot{\gamma}(\mathbf{u})$ and $\tau(\mathbf{u})$, respectively, are

$$\dot{\gamma}(\mathbf{u}) = \left[\frac{1}{2} \sum_{i,j=1}^3 [\dot{\gamma}_{ij}(\mathbf{u})]^2 \right]^{1/2}, \quad \tau(\mathbf{u}) = \left[\frac{1}{2} \sum_{i,j=1}^3 [\tau_{ij}(\mathbf{u})]^2 \right]^{1/2}. \quad (5)$$

The two dimensionless parameters appearing above are the Reynolds number, Re , and the Bingham number, B , which are defined by

$$Re = \frac{\hat{\rho} \hat{R} \hat{U}_0}{\hat{\mu}}, \quad B = \frac{\hat{\tau}_Y \hat{R}}{\hat{U}_0 \hat{\mu}}. \quad (6)$$

Here, $\hat{\rho}$ is the fluid density, \hat{R} the pipe radius (or $2\hat{R}$ the separation of the parallel plates), \hat{U}_0 the mean axial velocity, $\hat{\mu}$ the plastic viscosity and $\hat{\tau}_Y$ the yield stress. The axis of the ducts is aligned with the z -coordinate and the walls are at $y = \pm 1$ (plane channel), or $r = 1$ (pipe). To derive (1) and (2), we have scaled lengths with \hat{R} , velocity with \hat{U}_0 , time with \hat{R}/\hat{U}_0 , modified pressure with $\hat{\rho} \hat{U}_0^2$ and deviatoric stress with $\hat{\mu} \hat{U}_0 / \hat{R}$.

2.1. Basic flows

It is straightforward to derive the Bingham–Poiseuille flow solutions that we later perturb. For one-dimensional shear flows, the pressure does not vary across the ducts, only one component of the deviatoric stress is non-zero and only the axial component of velocity W is non-zero, depending only on

distance from the duct walls. The velocity profiles are

$$W(y) = \begin{cases} \frac{B}{2y^*}(1 - y^*)^2, & 0 \leq |y| \leq y^*, \\ \frac{B}{2y^*}[(1 - y^*)^2 - (|y| - y^*)^2], & y^* < |y| \leq 1, \end{cases} \quad (7)$$

$$W(r) = \begin{cases} \frac{B}{2r^*}(1 - r^*)^2, & 0 \leq r \leq r^*, \\ \frac{B}{2r^*}[(1 - r^*)^2 - (r - r^*)^2], & r^* < r \leq 1, \end{cases} \quad (8)$$

where y^* and r^* denote the positions of the yield surfaces. Since the mean velocity has been used to scale the flow, it follows that

$$1 = \int_0^1 W(y) dy, \quad 1 = 2 \int_0^1 rW(r) dr, \quad (9)$$

for the plane channel and pipe. After some relatively simple algebra, it can be shown that

$$0 = (y^*)^3 - 3y^* \left[1 + \frac{2}{B} \right] + 2, \quad (10)$$

for the plane channel and

$$0 = (r^*)^4 - 4r^* \left[1 + \frac{3}{B} \right] + 3, \quad (11)$$

for the pipe. Having found y^* and r^* , the magnitude of the axial pressure gradient is related to the yield surface positions by

$$y^* = \frac{B}{Re|(dp/dz)|}, \quad r^* = \frac{2B}{Re|(dp/dz)|} \quad (12)$$

and the solution is complete.

The polynomial (10) has three real roots. The solution is that which satisfies $0 < y^* < 1$. The polynomial (11) has four roots: two are real and two are complex conjugates. The solution is the real root which satisfies the condition $0 < r^* < 1$. Eq. (11) is originally due to Buckingham. It is straightforward to compute the roots of (10) and (11) numerically. As $B \rightarrow 0$, the functions $y^*(B)$ and $r^*(B)$ tend to 0:

$$y^* \sim \frac{1}{3}B - \frac{1}{6}B^2 \quad \text{as } B \rightarrow 0, \quad r^* \sim \frac{1}{4}B - \frac{1}{12}B^2 \quad \text{as } B \rightarrow 0. \quad (13)$$

Later, we will be interested in the limit $B \rightarrow \infty$, in which the unyielded plug regions widen towards the walls. An asymptotic expansion for large B gives the following expressions:

$$y^*(B) \sim 1 - \frac{\sqrt{2}}{B^{1/2}} + \frac{2}{3B} + O(B^{-3/2}), \quad (14)$$

$$r^*(B) \sim 1 - \frac{\sqrt{2}}{B^{1/2}} + \frac{1}{3B} + O(B^{-3/2}). \quad (15)$$

Fig. 1 shows the asymptotic expressions $r^*(B)$ and $y^*(B)$ plotted against the numerical solution.

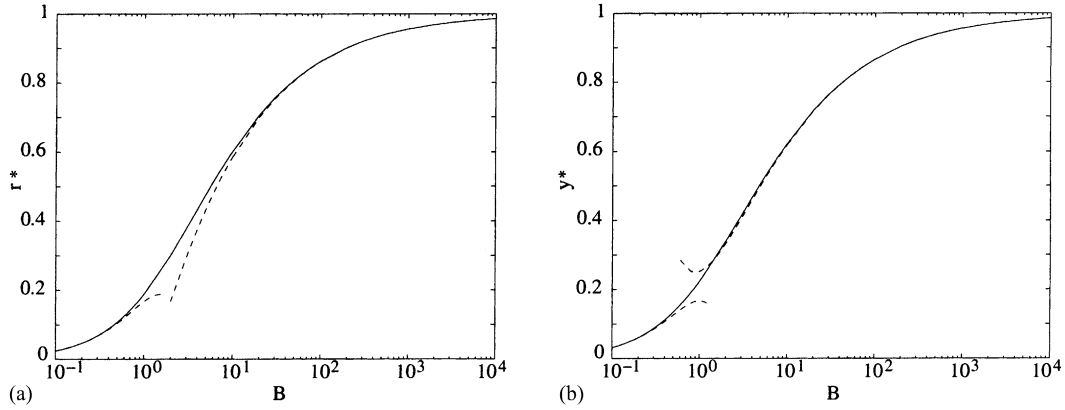


Fig. 1. The roots of Buckingham’s polynomials for pipe and channel —(a) pipe: $r^*(B)$; (b) plane channel: $y^*(B)$. The dashed lines show asymptotic expansions to $r^*(B)$ and $y^*(B)$, valid for large and small B .

3. Nonlinear stability

Nonlinear stability results do not appear to have been derived previously for the Bingham–Poiseuille flows that we consider. Our objectives are two-fold. First, to derive rigorous global stability bounds, that show a variation with B . These bounds provide a lower bound on the critical Reynolds number needed for transition. Second, we improve on these bounds, for conditional stability. We consider in detail the plane channel flow, stating the analogous results for the pipe flow afterwards.

3.1. Preliminaries

Our approach is classical and our main tool will be the Reynolds–Orr energy equation. This equation is straightforwardly derived from the Navier–Stokes equations (see, for example in [8]). Let Ω denote the part of the duct (plane channel or pipe) under consideration and let $\partial\Omega$ denote the walls. Denote by $\mathbf{U} = (0, 0, W)^T$, the basic flow of Section 2.1. We consider the evolution of an arbitrary perturbation $\mathbf{u} = (u, v, w)^T$ to the basic flow. Denote by $H(t)$, the dimensionless mean kinetic energy of the perturbation:

$$H(t) = \frac{1}{\|\Omega\|} \int_{\Omega} \frac{|\mathbf{u}|^2}{2} d\Omega = \frac{1}{\|\Omega\|} \int_{\Omega} \frac{u^2 + v^2 + w^2}{2} d\Omega. \tag{16}$$

We denote by $\langle \cdot \rangle$, the operation of integrating over Ω and dividing by the area $\|\Omega\|$ of Ω , i.e. $H(t) \equiv \langle |\mathbf{u}|^2 \rangle / 2$. For the plane channel flow, the Reynolds–Orr equation is

$$\frac{d}{dt} H(t) = - \left\langle v w \frac{dW}{dy} \right\rangle - \frac{1}{Re} \left\langle \frac{1}{2} [\tau_{ij}(\mathbf{U} + \mathbf{u}) - \tau_{ij}(\mathbf{U})] \dot{\gamma}_{ij}(\mathbf{u}) \right\rangle. \tag{17}$$

For the pipe flow, the velocity components in (r, θ, z) -directions are denoted (u, v, w) and the corresponding equation is

$$\frac{d}{dt} H(t) = - \left\langle u w \frac{dW}{dr} \right\rangle - \frac{1}{Re} \left\langle \frac{1}{2} [\tau_{ij}(\mathbf{U} + \mathbf{u}) - \tau_{ij}(\mathbf{U})] \dot{\gamma}_{ij}(\mathbf{u}) \right\rangle. \tag{18}$$

For the manipulations that follow, we assume that Ω has an arbitrarily large length in any direction for which the duct is infinite. It is assumed that each of the integrals in (16)–(18) (and all equations that follow), exist as $|\Omega| \rightarrow \infty$. We choose our class of perturbations accordingly.

For the plane channel, we denote by $D_{\text{channel}}(\Omega)$, the set of C^∞ functions having support that is compact in the y -direction, i.e. across the channel, and which are almost periodic in the x - and z -directions. For such functions, the integrals in (16)–(18) are well defined as $|\Omega| \rightarrow \infty$. We define V_0 and \bar{V}_0 by

$$V_0 = \{ \mathbf{v} : \mathbf{v} \in D_{\text{channel}}(\Omega)^3, \nabla \cdot \mathbf{v} = 0 \text{ in } \Omega, \mathbf{v} = 0 \text{ in } \partial\Omega \}, \quad (19)$$

$$\bar{V}_0 = \text{closure of } V_0 \text{ w.r.t. } \|\cdot\|_{H^1(\Omega)} : \|\mathbf{v}\|_{H^1(\Omega)} = \left\langle v_j v_j + \frac{\partial v_i}{\partial x_j} \frac{\partial v_i}{\partial x_j} \right\rangle. \quad (20)$$

We assume that the following identity holds for $\mathbf{v} \in \bar{V}_0$:

$$\langle \dot{\gamma}^2(\mathbf{v}) \rangle = \left\langle \frac{\partial v_i}{\partial x_j} \frac{\partial v_i}{\partial x_j} \right\rangle, \quad (21)$$

taking the limit as $|\Omega| \rightarrow \infty$, in the case of an almost periodic function, to eliminate the boundary integral remainders. Note that if $\mathbf{v} \in V_0$, then Eq. (21) is satisfied straightforwardly on integrating by parts.

Remarks. We consider \bar{V}_0 as the test space for our initial perturbations of the basic flow. The general approach is to consider arbitrary initial conditions for the perturbation $\mathbf{U} + \mathbf{u}$ and derive conditions under which all such perturbations decay monotonically. We are not concerned with regularity of the solutions with respect to t , and simply assume sufficient regularity for whatever follows. Thus, our approach should be considered purely formal. For the stability analysis to make sense, the function $\mathbf{U} + \mathbf{u}$ will be a solution to a three-dimensional Bingham fluid flow problem in an infinite duct. However, we know of no results that actually establish existence and uniqueness of a solution to this problem for three-dimensional infinite domains (see [9] and the improved results in [10] for finite three-dimensional interior domains). A second reason for a purely formal approach is that, even assuming the existence and uniqueness of our perturbed velocities, the properties of solutions of Bingham flow problems are not well established at a rigorous level in three-dimensions. In two-dimensions, this is not the case and we can refer to Duvaut and Lions [9], and to the stronger results established later by Kim [11].

To treat the pipe flow, we denote by $D_{\text{pipe}}(\Omega)$ the set of C^∞ functions having support that is compact in the r -direction (i.e. meaning that they vanish near the pipe wall), which are almost periodic in the z -direction and which are periodic with period 2π in the θ -direction. The spaces V_0 and \bar{V}_0 are then defined analogously.

3.2. Dissipation terms

We rewrite the dissipation term in (17) by putting

$$-\langle \frac{1}{2} [\tau_{ij}(\mathbf{U} + \mathbf{u}) - \tau_{ij}(\mathbf{U})] \dot{\gamma}_{ij}(\mathbf{u}) \rangle = \langle I(\mathbf{U}, \mathbf{u}) \rangle \quad (22)$$

and consider the integrand $I(\mathbf{U}, \mathbf{u})$ in different regions of the flow. Considering the basic and perturbed flows, we note that at any fixed time the domain Ω can be subdivided into four distinct regions (not necessarily simply connected).

1. Region A, where both the basic and perturbed flows are unyielded: $\tau(\mathbf{U}) \leq B$ and $\tau(\mathbf{U} + \mathbf{u}) \leq B$ in region A.
2. Region B, where the basic flow is unyielded, but the perturbed flow is yielded: $\tau(\mathbf{U}) \leq B$ and $\tau(\mathbf{U} + \mathbf{u}) > B$ in region B.
3. Region C, where the basic flow is yielded, but the perturbed flow is unyielded: $\tau(\mathbf{U}) > B$ and $\tau(\mathbf{U} + \mathbf{u}) \leq B$ in region C.
4. Region D, where both basic and perturbed flows are yielded: $\tau(\mathbf{U}) > B$ and $\tau(\mathbf{U} + \mathbf{u}) > B$ in region D.

In region A, both flows are unyielded, $\dot{\gamma}_{ij}(\mathbf{u}) = 0, \forall i, j$, and trivially:

$$0 = I(\mathbf{U}, \mathbf{u}) \leq -\dot{\gamma}^2(\mathbf{u}) = 0. \quad (23)$$

In region B, we have $\dot{\gamma}(\mathbf{U}) = 0$ and also $\dot{\gamma}(\mathbf{U} + \mathbf{u}) = \dot{\gamma}(\mathbf{u})$ since

$$\dot{\gamma}(\mathbf{U} + \mathbf{u}) = |\dot{\gamma}(\mathbf{U} + \mathbf{u}) - \dot{\gamma}(\mathbf{U})| \leq \dot{\gamma}(\mathbf{U} + \mathbf{u} - \mathbf{U}) = \dot{\gamma}(\mathbf{u}),$$

$$\dot{\gamma}(\mathbf{u}) = \dot{\gamma}(\mathbf{U} + \mathbf{u} - \mathbf{U}) \leq |\dot{\gamma}(\mathbf{U} + \mathbf{u}) + \dot{\gamma}(\mathbf{U})| = \dot{\gamma}(\mathbf{U} + \mathbf{u}).$$

Therefore,

$$\begin{aligned} I(\mathbf{U}, \mathbf{u}) &\leq - \left[1 + \frac{B}{\dot{\gamma}(\mathbf{U} + \mathbf{u})} \right] \frac{1}{2} \dot{\gamma}_{ij}(\mathbf{U} + \mathbf{u}) \dot{\gamma}_{ij}(\mathbf{u}) + B \dot{\gamma}(\mathbf{u}) \\ &\leq - \left[1 + \frac{B}{\dot{\gamma}(\mathbf{u})} \right] \frac{1}{2} \dot{\gamma}_{ij}(\mathbf{u}) \dot{\gamma}_{ij}(\mathbf{u}) + B \dot{\gamma}(\mathbf{u}) = -\dot{\gamma}^2(\mathbf{u}). \end{aligned} \quad (24)$$

Similarly, in region C, we have $\dot{\gamma}(\mathbf{U} + \mathbf{u}) = 0$ and $\dot{\gamma}(\mathbf{U}) = \dot{\gamma}(\mathbf{u})$, which leads to

$$\begin{aligned} I(\mathbf{U}, \mathbf{u}) &\leq B \dot{\gamma}(\mathbf{u}) + \left[1 + \frac{B}{\dot{\gamma}(\mathbf{U})} \right] \frac{1}{2} \dot{\gamma}_{ij}(\mathbf{U} + \mathbf{u} - \mathbf{u}) \dot{\gamma}_{ij}(\mathbf{u}) \\ &\leq B \dot{\gamma}(\mathbf{u}) - \left[1 + \frac{B}{\dot{\gamma}(\mathbf{u})} \right] \frac{1}{2} \dot{\gamma}_{ij}(\mathbf{u}) \dot{\gamma}_{ij}(\mathbf{u}) = -\dot{\gamma}^2(\mathbf{u}). \end{aligned} \quad (25)$$

Finally, in region D, both flows are yielded and we have

$$\begin{aligned} I(\mathbf{U}, \mathbf{u}) &= - \left[1 + \frac{B}{\dot{\gamma}(\mathbf{U} + \mathbf{u})} \right] \frac{1}{2} \dot{\gamma}_{ij}(\mathbf{U} + \mathbf{u}) \dot{\gamma}_{ij}(\mathbf{U} + \mathbf{u} - \mathbf{U}) \\ &\quad + \left[1 + \frac{B}{\dot{\gamma}(\mathbf{U})} \right] \frac{1}{2} \dot{\gamma}_{ij}(\mathbf{U}) \dot{\gamma}_{ij}(\mathbf{U} + \mathbf{u} - \mathbf{U}) \leq -\dot{\gamma}^2(\mathbf{u}), \end{aligned} \quad (26)$$

by using the Cauchy–Schwarz inequality on the terms multiplied by B . Therefore, considering all regions together and using (21):

$$\langle I(\mathbf{U}, \mathbf{u}) \rangle \leq \langle \dot{\gamma}^2(\mathbf{u}) \rangle = \left\langle \frac{\partial u_i}{\partial x_j} \frac{\partial u_i}{\partial x_j} \right\rangle. \quad (27)$$

This expression is identical for the pipe geometry.

3.3. *Global stability bounds*

Substituting from the basic solution in Section 2.1, the inertial term in (17) is

$$-\int_{\Omega} \frac{dW}{dy} v w \, d\Omega = \frac{B}{y^*} \int_{\Omega(y^*)} \sin(y)(|y| - y^*) v w \, d\Omega \leq \frac{(1 - y^*)B}{2y^*} \int_{\Omega(y^*)} (v^2 + w^2) \, d\Omega, \tag{28}$$

where $\Omega(y^*)$ denotes the region $|y| > y^*$. Assuming $y > y^*$:

$$v^2 = \left[\int_1^y \frac{\partial v}{\partial s}(x, s, z, t) \, ds \right]^2 \leq (1 - y^*) \int_{y^*}^1 \left[\frac{\partial v}{\partial s}(x, s, z, t) \right]^2 \, ds, \tag{29}$$

using the Cauchy–Schwarz inequality. Treating $y < -y^*$ and w^2 similarly, and then interchanging the y -integration:

$$\int_{\Omega(y^*)} [v^2 + w^2] \, d\Omega \leq (1 - y^*)^2 \int_{\Omega} \frac{\partial u_i}{\partial x_j} \frac{\partial u_i}{\partial x_j} \, d\Omega. \tag{30}$$

Combining this with our bound for the dissipative terms, we have

$$\frac{d}{dt} H(t) \leq - \left[\frac{1}{Re} - \frac{B(1 - y^*)^3}{2y^*} \right] \left\langle \frac{\partial u_i}{\partial x_j} \frac{\partial u_i}{\partial x_j} \right\rangle. \tag{31}$$

Thus, the energy of an arbitrary initial perturbation decreases monotonically provided that

$$Re < Re_{GB} = \frac{2y^*}{B(1 - y^*)^3}. \tag{32}$$

For the pipe, the manipulations are similar and lead to

$$\frac{d}{dt} H(t) \leq - \left[\frac{1}{Re} - \frac{B(1 - r^*)^3(1 + r^*)}{4(r^*)^2} \right] \left\langle \frac{\partial u_i}{\partial x_j} \frac{\partial u_i}{\partial x_j} \right\rangle \tag{33}$$

and the energy of an arbitrary initial perturbation decreases monotonically provided that

$$Re < Re_{GB} = \frac{4(r^*)^2}{B(1 - r^*)^3(1 + r^*)}. \tag{34}$$

It is evident that the bounds (32) and (33) are not at all sharp. Indeed, (34) vanishes as $B \rightarrow 0$, and (32) becomes $Re < 2/3$. Much stronger energy bounds are available for the analogous Newtonian flows. However, it is the behaviour as $B \rightarrow \infty$ that is our primary interest. Using (14) and (15), we have

$$Re_{GB} \sim \sqrt{\frac{1}{2}B} \quad \text{as } B \rightarrow \infty, \tag{35}$$

for both the plane channel and pipe. Note that Re_{GB} is a lower bound for the Reynolds number below which the flows are globally and monotonically stable. Although clearly a very weak approximation to the true bound for global stability, Re_{GB} shows that for a sufficiently large B a Bingham fluid flow will be more stable than the corresponding Newtonian fluid flow, obtained by setting $B = 0$. This fact has not been previously established, although it is a common experimental observation.

3.4. Conditional stability

Our main purpose in deriving (32) and (34) has been to show that a bound of form $Re \sim B^{1/2}$ as $B \rightarrow \infty$ can be rigorously established for arbitrary sized perturbations. In order to improve the bounds (32) and (34), we restrict the size of admissible perturbations as follows:

$$|\tau_{ij}(\mathbf{U} + \mathbf{u}) - \tau_{ij}(\mathbf{U})| \leq a, \quad (36)$$

where a is a constant parameter, to be defined later. We note that it is exactly this type of bound that is necessary in order to develop a linear stability theory. Now, we select a in order to ensure that there remains an unyielded region of fluid for the perturbed flow. Results for the pipe will be stated later, but follow the same derivation. From (36) and the basic flows, we deduce that

$$|\tau_{ij}(\mathbf{U} + \mathbf{u})| \leq a, \quad ij \neq yz, zy, \quad (37)$$

$$|f|y| - a| \leq |\tau_{ij}(\mathbf{U} + \mathbf{u})| \leq f|y| + a, \quad ij = yz, zy, \quad (38)$$

and therefore,

$$|f|y| - a| \leq \tau(\mathbf{U} + \mathbf{u}) = \left[\frac{1}{2} \sum_{i,j=1}^3 \tau_{ij}^2(\mathbf{U} + \mathbf{u}) \right]^{1/2} \leq [(f|y| + a)^2 + \frac{7}{2}a^2]^{1/2}. \quad (39)$$

We now select a and y such that the upper bound satisfies

$$(f|y| + a)^2 + \frac{7}{2}a^2 < B^2 = (fy^*)^2,$$

i.e. assuring that $\tau(\mathbf{U} + \mathbf{u}) < B$. Defining $\beta = a/f$, we see that the disturbed flow must be unyielded provided that $|y| < y_2$, which is the larger root of

$$(f|y| + a)^2 + \frac{7}{2}a^2 - (fy^*)^2 = 0,$$

$$y_2 = -\beta + \sqrt{(y^*)^2 - \frac{7}{2}\beta^2}. \quad (40)$$

We require both that the discriminant above is positive and that $y_2 > 0$. These constraints are satisfied if

$$y^* > \frac{3}{\sqrt{2}}\beta \Leftrightarrow \frac{a}{B} < \frac{\sqrt{2}}{3}. \quad (41)$$

We define the layer thickness h by

$$-h = y_2 - y^*. \quad (42)$$

Note in passing that $h > \beta$, and that

$$h \sim \beta + y^* \frac{7}{4} \left(\frac{a}{B} \right)^2 + O \left(\left(\frac{a}{B} \right)^4 \right) \quad \text{as } B \rightarrow \infty. \quad (43)$$

Therefore, finally we have that

$$\tau(\mathbf{U} + \mathbf{u}) \leq B, \quad \text{if } |y| \leq y^* - h, \quad (44)$$

$$\tau(\mathbf{U} + \mathbf{u}) > B, \quad \text{if } |y| > y^* + h. \quad (45)$$

Returning to the energy equation (Eq. (17)) and the bounds derived for the dissipative terms, we see that regions B, C, and D are contained in the region, $\Omega(y_2) : y_2 \leq |y| \leq 1$. Secondly, since region A makes no contribution to the total dissipation functional, we have

$$\int_{\Omega} I(\mathbf{U}, \mathbf{u}) \, d\Omega \leq - \int_{\Omega} \dot{\gamma}^2(\mathbf{u}) \, d\Omega = - \int_{\Omega} \frac{\partial u_i}{\partial x_j} \frac{\partial u_i}{\partial x_j} \, d\Omega = - \int_{\Omega(y_2)} \frac{\partial u_i}{\partial x_j} \frac{\partial u_i}{\partial x_j} \, d\Omega. \quad (46)$$

The inertial term in (17), we treat as follows:

$$\begin{aligned} - \int_{\Omega} v w \frac{dW}{dy} \, d\Omega &= \frac{B}{y^*} \int_{\Omega(y^*)} \sin(y)(|y| - y^*) v w \, d\Omega \\ &= \frac{B}{y^*} \int_{\Omega(y_2)} \sin(y)(|y| - y_2) v w \, d\Omega - \frac{B}{y^*} \int_{\Omega(y_2)} g(y) v w \, d\Omega, \end{aligned} \quad (47)$$

where $g(y)$ is the function:

$$g(y) = \begin{cases} \sin(y)(y^* - y_2), & y^* \leq |y| \leq 1, \\ \sin(y)(|y| - y_2), & y_2 \leq |y| \leq y^*. \end{cases} \quad (48)$$

The first term on the right-hand side of (47), we bound by

$$\int_{\Omega(y_2)} \sin(y)(|y| - y_2) v w \, d\Omega \leq \Lambda \int_{\Omega(y_2)} \frac{\partial u_i}{\partial x_j} \frac{\partial u_i}{\partial x_j} \, d\Omega, \quad (49)$$

where Λ is given by

$$\Lambda = \sup_{\mathbf{v} \in \bar{V}_0^*} \left[\frac{\int_{\Omega(y_2)} \sin(y)(|y| - y_2) v_2 v_3 \, d\Omega}{\int_{\Omega(y_2)} (\partial v_i / \partial x_j)(\partial v_i / \partial x_j) \, d\Omega} \right] \quad (50)$$

and where \bar{V}_0^* is the subset of \bar{V}_0 satisfying

$$\frac{\partial v_i}{\partial x_j}(x, y, z, t) = 0, \quad |y| \leq y_2, \quad \forall i, j, \quad (51)$$

i.e. since the region $|y| \leq y_2$ is unyielded. We now map the region $y_2 \leq |y| \leq 1$ back onto the full channel Ω , using the following simple transformation:

$$\tilde{x}(1 - y_2) = x, \quad \tilde{z}(1 - y_2) = z, \quad \tilde{y}(1 - y_2) = \sin(y)(|y| - y_2). \quad (52)$$

We have that

$$\frac{\int_{\Omega(y_2)} \sin(y)(|y| - y_2) v_2 v_3 \, d\Omega}{\int_{\Omega(y_2)} (\partial v_i / \partial x_j)(\partial v_i / \partial x_j) \, d\Omega} = (1 - y_2)^3 \frac{\int_{\Omega} v_2 v_3 \tilde{y} \, d\Omega}{\int_{\Omega} (\partial v_i / \partial \tilde{x}_j)(\partial v_i / \partial \tilde{x}_j) \, d\Omega}. \quad (53)$$

Note that this transformation has essentially no effect in the x - and z -directions, since the domain is considered infinite in those directions. Secondly, since (51) holds at $|y| = y_2 \mapsto \tilde{y} = 0$, the transformed

vector \mathbf{v} will be differentiable at $\tilde{y} = 0$ and \mathbf{v} will simply take the values of the velocity of the unyielded central plug region, i.e. \mathbf{v} remains well defined at $\tilde{y} = 0$ after the transformation. Condition (51) becomes

$$\frac{\partial v_i}{\partial \tilde{x}_j}(\tilde{x}, 0, \tilde{z}, t) = 0, \quad \forall i, j. \tag{54}$$

Relaxing (54), it follows that

$$\Lambda \leq (1 - y_2)^3 \max_{\mathbf{v} \in \bar{V}_0^*} \left[\frac{\int_{\Omega} v_2 v_3 \tilde{y} \, d\Omega}{\int_{\Omega} (\partial v_i / \partial \tilde{x}_j)(\partial v_i / \partial \tilde{x}_j) \, d\Omega} \right] = \frac{(1 - y_2)^3}{2Re_{\text{Busse}}}. \tag{55}$$

The value for the constant is $Re_{\text{Busse}} = 99.207$, as first obtained by Busse [6], in his derivation of an energy stability bound for plane Poiseuille flow of a Newtonian fluid. For the second term on the right-hand side of (47), we proceed with the same crude method as for the global stability. Omitting the details, we arrive at

$$\int_{\Omega(y_2)} g(y)vw \, d\Omega \leq \frac{h(1 - y_2)^2}{2} \int_{\Omega(r_2)} \frac{\partial u_i}{\partial x_j} \frac{\partial u_i}{\partial x_j} \, d\Omega. \tag{56}$$

We note that the constant multiplying $h(1 - y_2)^2$ could be improved, but we would retain terms in our stability bound (below) that are $O(h)$ as $B \rightarrow \infty$. Combining our bounds, we arrive finally at

$$\frac{d}{dt}H(t) \leq - \left[\frac{1}{Re} - \frac{B(1 - y_2)^3}{2y^*Re_{\text{Busse}}} - \frac{hB(1 - y_2)^2}{2y^*} \right] \left\langle \frac{\partial u_i}{\partial x_j} \frac{\partial u_i}{\partial x_j} \right\rangle. \tag{57}$$

We now select h to satisfy (41). We set h as

$$h = \frac{\sqrt{2} y^*(1 - y^*)}{3 Re_{\text{Busse}}}. \tag{58}$$

Consequently, perturbations of size

$$|\tau_{ij}(\mathbf{U} + \mathbf{u}) - \tau_{ij}(\mathbf{U})| \leq a \leq \frac{\sqrt{2} B(1 - y^*)}{3 Re_{\text{Busse}}} \tag{59}$$

will decay monotonically provided that $Re < Re_{\text{CB}}$, where the conditional bound Re_{CB} is given by

$$Re_{\text{CB}} = \frac{2y^*Re_{\text{Busse}}/B(1 - y^*)^3}{[1 + (\sqrt{2}/3)(y^*/Re_{\text{Busse}})]^2 [1 + (\sqrt{2}/3)y^* + (\sqrt{2}/3)(y^*/Re_{\text{Busse}})]}. \tag{60}$$

Our chief interest is the behaviour for large B . Using (14), we have

$$Re_{\text{CB}} \sim \frac{\sqrt{B/2} Re_{\text{Busse}}}{[1 + (\sqrt{2}/3 Re_{\text{Busse}})]^2 [1 + (\sqrt{2}/3) + (\sqrt{2}/3 Re_{\text{Busse}})]}. \tag{61}$$

Remarks.

1. The conditional stability bound (60) is certainly still conservative, as is to be expected from the analogous Newtonian results, where one order of magnitude separates global stability bounds and

actual transition. Although (60) is a conditional bound, bounds on the size of perturbation are not restrictive. As $B \rightarrow \infty$, we have $|\tau_{ij}(\mathbf{U} + \mathbf{u}) - \tau_{ij}(\mathbf{U})| \leq a \sim B^{1/2}$, implying that $\dot{\gamma}(\mathbf{u}) \sim B^{1/2}$, and the width of yielded region $[1 - y_2] \sim 1/B^{1/2}$. Thus, we can allow $\|\mathbf{u}\| \sim 1$ for our perturbations, i.e. not necessarily weak perturbations. If, instead, we were to restrict $h \sim O(1/B^{1/2})$ as $B \rightarrow \infty$, we could improve to $Re_{CB} \sim \sqrt{B/2} Re_{Busse}$, but our perturbations will also be $\|\mathbf{u}\| \sim O(1)$ as $B \rightarrow \infty$. Similarly, allowing say $h \sim B^{-\nu}$ for $1/3 < \nu < 1/2$ will allow stability to perturbations with $\|\mathbf{u}\| \sim B^{1-2\nu}$ for a conditional bound $Re_{CB} \sim B^{3\nu-1}$, which is worse than the global stability result.

2. With regard to the above remark, our choice $h \sim 1/B^{1/2}$ is perhaps the most practical. Objectively, when we consider transition of shear flows such as these, we are most interested in when the flow is or is not stable to $O(1)$ perturbations, i.e. a perturbation that is larger than $O(1)$ is *unnatural*, but a perturbation that is $O(1)$ as $B \rightarrow \infty$ is only weakly nonlinear. Our conditional stability results are valid for strongly nonlinear perturbations.
3. A second question is whether we can improve the bound numerically, whilst retaining the estimate $h \sim 1/B^{1/2}$. In fact this seems possible with a little more care. Typically, the components v_2 and v_3 of the functions \mathbf{v} that maximise expressions such as (55) are such that the integrand $v_2 v_3 \tilde{y}$ is non-negative everywhere (see, for example, Fig. 2 in [6]), where v_2 is anti-symmetric and v_3 symmetric, with respect to the channel centreline. Assuming that this assumption can be made a priori, then the second integral on the right-hand side of (47) will be positive and can be neglected. Repeating the above analysis, we can derive a bound of form

$$Re_{CB} = \frac{2y^* Re_{Busse} / B(1 - y^*)^3}{[1 + (\delta y^* \sqrt{2}/3)]^3}, \quad \text{for any } \delta \in (0, 1), \tag{62}$$

with conditional bound

$$|\tau_{ij}(\mathbf{U} + \mathbf{u}) - \tau_{ij}(\mathbf{U})| \leq a \leq \frac{1}{3}[\delta B(1 - y^*)\sqrt{2}]. \tag{63}$$

Thus, again we have the trade-off between size of (order unity) perturbation and growth in the bound.

4. An alternative strategy is to directly treat the Euler equations corresponding to the maximisation:

$$\Lambda = \sup_{\mathbf{v} \in \bar{V}_0^*} \left[\frac{\int_{\Omega(y_2)} (dW/dy) v w \, d\Omega}{\int_{\Omega(y_2)} (\partial v_i / \partial x_j) (\partial v_i / \partial x_j) \, d\Omega} \right]. \tag{64}$$

There is a small technical problem here, since $dW/dy = 0$ for $y \in [y_2, y^*]$, so that the maximisers will not be unique. However, this can be neglected in the limit $B \rightarrow \infty$ if $h \rightarrow 0$, as above. To consider the correct Bingham fluid problem is then a purely mathematical exercise, which we do not expect to lead to results that are an order of magnitude closer to the values for transition. Having said this, the inclusion of (54) as a constraint should improve the bound, we have used (note that Busse’s minimising eigenfunctions in [6] do not satisfy (54)).

5. Treating the pipe flow analogously to the channel, the energy bound is

$$\frac{d}{dt} H(t) \leq - \left[\frac{1}{Re} - \frac{B(1 - r_2)^3}{2r^* Re_{Joseph}} - \frac{hB(1 - r_2)^2(1 + r_2)}{4r^* r_2} \right] \left\langle \frac{\partial u_i}{\partial x_j} \frac{\partial u_i}{\partial x_j} \right\rangle,$$

where $Re_{Joseph} \approx 81.49$ is Joseph’s approximate value for the energy stability of Hagen–Poiseuille

flow (which we assume to be the minimal value) [7]. Selection of h is analogous,

$$h = \frac{\sqrt{2} r^* (1 - r^*)}{3 Re_{\text{Joseph}}} \quad (65)$$

and then perturbations of size

$$|\tau_{ij}(\mathbf{U} + \mathbf{u}) - \tau_{ij}(\mathbf{U})| \leq a \leq \frac{\sqrt{2} B (1 - r^*)}{3 Re_{\text{Joseph}}} \quad (66)$$

will decay monotonically provided that $Re < Re_{\text{CB}}$, where the conditional bound Re_{CB} is given by

$$Re_{\text{CB}} = \frac{2r^* Re_{\text{Joseph}} / B (1 - r^*)^3}{[1 + (\sqrt{2}/3)(r^*/Re_{\text{Joseph}})]^2 [1 + (\sqrt{2}/3)((1 + r_2)/2r_2) + (\sqrt{2}/3)(r^*/Re_{\text{Joseph}})]}. \quad (67)$$

Again, as $B \rightarrow \infty$:

$$Re_{\text{CB}} \sim \frac{\sqrt{B/2} Re_{\text{Joseph}}}{[1 + (\sqrt{2}/3 Re_{\text{Joseph}})]^2 [1 + (\sqrt{2}/3) + (\sqrt{2}/3 Re_{\text{Joseph}})]}. \quad (68)$$

Most of the comments made above for the plane channel stability bounds and possible improvements on the bounds can also be repeated for the pipe.

3.5. Linear stability

There are no results for linear stability of Poiseuille flow of a Bingham fluid in a pipe. However, the corresponding Newtonian fluid flow is thought to be to be linearly stable (see [2–5]), and we assume that the same will also be true of the Bingham fluid flow. Two-dimensional linear stability of plane Poiseuille flow of a Bingham fluid is considered in [1] and is governed by the following Orr–Sommerfeld eigenvalue problem:

$$\begin{aligned} & i\alpha Re^* [(1 - \xi^2 - c)(\phi_{\xi\xi} - \alpha^2 \phi) + 2\phi] \\ & = \left[\frac{d^2}{d\xi^2} - \alpha^2 \right]^2 \phi - 4\alpha^2 B^* \frac{d}{d\xi} \left[\frac{\phi_\xi}{\xi} \right], \quad \text{for } \xi \in (0, 1), \end{aligned} \quad (69)$$

with boundary conditions:

$$\phi(0) = \phi_\xi(0) = 0, \quad (70)$$

$$\phi(1) = \phi_\xi(1) = 0, \quad (71)$$

$$\phi_{\xi\xi}(0) - \alpha^2 \phi(0) = 2h. \quad (72)$$

Here, the Reynolds number Re^* and Bingham number B^* are defined using the maximum velocity of the basic flow and are scaled with the width of the yielded flow region. This eigenvalue problem has been solved numerically in [1], to determine the marginal stability curves for different values of B^* . From these curves, a minimal Reynolds number Re_{lin}^* for linear instability can be computed. Fig. 2a shows the results of these computations for $B^* \in [0, 4000]$. Fig. 2b shows the critical Reynolds number Re_{lin} , for

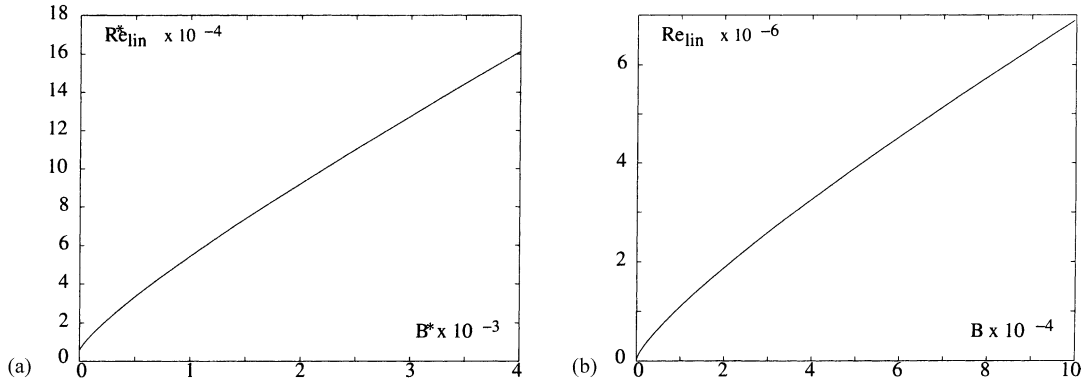


Fig. 2. (a) The critical Reynolds number for instability to two-dimensional linear disturbances, $Re_{lin}^*(B^*)$, as computed in [1]. (b) The critical Reynolds number $Re_{lin}(B)$.

linear instability, expressed as a function of B , after the relevant transformations from Re^* and B^* to Re and B . It is apparent that Re_{lin} increases approximately linearly with B for large B . By numerically differentiating the data points, we can estimate the gradient of $Re_{lin}(B)$ at large B (i.e. up to the limit to which we have computed, $B \approx 8 \times 10^6$), giving

$$\frac{d}{dB} Re_{lin} \approx 36.9, \quad \text{at } B \approx 8 \times 10^6, \quad (73)$$

$$\frac{d^2}{dB^2} Re_{lin} \approx -3.5 \times 10^{-7}, \quad \text{at } B \approx 8 \times 10^6. \quad (74)$$

4. Phenomenological criteria

Laminar and turbulent flows of slurries and suspensions with Bingham fluid-like rheological behaviour are used for hydraulics applications in the petroleum and mining industries. Many phenomenological theories have been developed, chiefly to quantify the frictional pressure drop in different situations. These theories often also contain criteria that predict transition between laminar and turbulent regimes. We summarise below the principal approaches taken. In Section 4.1, we collate these expressions and examine the variation with B of each criteria.

4.1. Metzner and Reed

Metzner and Reed [12] used the Fanning friction factor F as their stability parameter. A range of data from pipe flow experiments with different non-Newtonian fluids indicated that the data deviated from the laminar flow curve, at approximately the same ratio of viscous shear to inertial forces as do Newtonian fluid data in smooth pipes, i.e. $F \approx 0.008$. They therefore proposed that for all time independent non-Newtonian fluids, transition would take place when F drops to a value of about 0.008 or less. Here, we have fixed the critical value at $F = F_c = 0.0076$, corresponding to a critical Reynolds number for the Newtonian flow of 2100.

The Metzner–Reed criterion is commonly applied in geometries other than circular pipes. For such geometries, a modified Reynolds number can be defined in such a way that in laminar flow, the friction factor relation is identical to that obtained for the pipe flow. Experimental studies using Newtonian fluid flowing through rectangular ducts of different aspect ratios [13], and through annular ducts of different radius ratio [14], show results broadly similar to the pipe flow, for both laminar and turbulent flows. In particular, the transition occurs at modified Reynolds number of ≈ 2000 , that is, $F \approx 0.008$. The Reynolds number defined by Metzner and Reed has thus been generalised by Kozicki et al. [15] to apply to laminar flows of purely viscous non-Newtonian fluids through ducts of arbitrary cross section. Experimental results obtained by Sourlier [16] and Kostic and Hartnett [17] for power law fluids flowing in rectangular ducts, demonstrate the utility of the modified Reynolds number as a hydraulic parameter and that the transition occurs at $F \approx 0.008$. The straightforward generalisation of Metzner and Reed's criterion is, therefore, to assume that for all purely viscous non-Newtonian fluids, transition would take place at $F = F_c = 0.0076$, independent of the duct geometry.

4.2. Hedström

According to Hedström [18], for given Hedström number $He = Re B$, transition occurs at the point of intersection of the laminar and turbulent friction factor curves. Hedström argues that for a fully turbulent fluid the effect of the yield stress is negligible and therefore uses the well known Nikuradse relation for the turbulent friction factor in the pipe. For the plane channel flow, based on the results of [13,14], a similar Nikuradse relation is assumed for the turbulent friction factor, but using a modified Reynolds number.

4.3. Local stability: Ryan and Johnson, Hanks

Two identical predictions of transitional Reynolds numbers have been made by Ryan and Johnson [19] and Hanks [20–22]. What is interesting is that these two predictions are arrived at using different approaches.

Ryan and Johnson [19] suggested to use the ratio of input energy to energy dissipation for an element of fluid as the stability parameter. They examine the situations in which the energy of a disturbance increases or decreases with time, considering the energy equation for a linear two-dimensional disturbance. The rate of increase of kinetic energy is equal to the difference between the rate at which energy is converted from the basic flow to the disturbance, via a Reynolds shear stress term. A ratio ζ is formed between the rate of increase and the rate at which energy is dissipated. The ratio ζ varies with radial position \hat{r} and thus their approach can be thought of as a *local* approach. It is assumed that transitional instabilities will first appear at the radial position where ζ is maximal, for all purely viscous non-Newtonian fluids. Further, it is assumed that instability occurs when this maximal value of ζ exceeds a critical number, ζ_{crit} , regardless of the exact fluid type. The critical number ζ_{crit} is defined from the transition of a Newtonian flow and is given by $\zeta_{crit} = 808$.

Hanks derives exactly the same criterion as Ryan and Johnson. However, his reasoning is different and more direct. Hanks identifies the key mechanism leading to transitional instability as being rotational momentum transfer. Hanks introduces a parameter, ζ_H , which is almost identical to that of Ryan and Johnson. However, for Hanks ζ_H represents a balance between the rate of change of angular momentum of a deforming fluid element and its rate of loss of momentum due to frictional drag. Hanks ratio ζ_H is exactly twice that of Ryan and Johnson. Hanks assumes that his transition criterion does not depend on

the constitutive equation, for purely viscous fluids, or on the geometry of flow. The value of $\zeta_{H,crit}$, where the laminar motion becomes unstable, was determined to be 404 when the theory was applied to axial isothermal Newtonian flow in tubes. The plane channel flow is considered, by analogous methods, in [21].

4.4. Integral stability: Mishra and Tripathi

Mishra and Tripathi [23] postulate that the important factors governing transition to turbulence are the mean kinetic energy and the wall shear stress. Furthermore, the onset of turbulence will occur at the same critical ratio of these quantities for all purely viscous non-Newtonian fluids. This ratio is fitted from its value for Newtonian fluid transition in a pipe. For the plane channel flow, we have generalised this approach using a modified Reynolds number.

4.4.1. Slatter's approach

A recent phenomenological approach is that due to Slatter [24]. He treats the unyielded region as a solid body which has no effect on the stability of flow. Therefore, only the flow of the sheared fluid in the *annulus*, between pipe wall and unyielded plug, is considered. Slatter defines a Reynolds number based on the effective viscosity of the annular flow, i.e. using the hydraulic diameter of the annulus and an effective rate of strain. Although Slatter has not considered a plane channel flow, we can easily extend his phenomenological reasoning to the plane channel flow. Slatter's approach to transition is not purely phenomenological and we discuss other contributions in Section 6.

4.5. Variation of Re_c with B

In the above sections, we have purposefully omitted algebraic details, since the different criteria have been formulated and expressed with a variety of different notations and dimensionless parameters. For purposes of comparison, we have expressed each of the phenomenological criteria in terms of our parameters R and B . These are shown in Table 1.

Notes.

1. Note that r^* and y^* are functions only of B in the above (see Fig. 1).

Table 1
Critical Reynolds according to the different phenomenological criteria

Criterion	Pipe flow	Plane channel
Metzner and Reed [12]	$Re_c = \frac{262.5B}{r^*}$	$Re_c = \frac{262.5B}{y^*}$
Ryan and Johnson [19], Hanks [20–22]	$Re_c = \frac{4200r^*}{B(1-r^*)^3}$	$Re_c = \frac{2100y^*}{B(1-y^*)^3}$
Hedström [18]	Compute numerically	Compute numerically
Mishra and Tripathi [23]	$Re_c = \frac{262.5B}{r^*C}$	$Re_c = \frac{405B}{y^*C}$
Slatter [24]	$Re_c = \frac{262.5(B+8W_{ann}/D_{ann})}{W_{ann}^2}$	$Re_c = \frac{262.5(B+12W_s/D_s)}{W_s^2}$

Table 2

Asymptotic behaviour of the different predictions of critical Reynolds numbers as $B \rightarrow \infty$

Criterion	Pipe flow	Plane channel
Metzner and Reed [12]	$Re_c \sim 262.5B + O(B^{1/2})$	$Re_c \sim 262.5B + O(B^{1/2})$
Ryan and Johnson [19], Hanks [20–22]	$Re_c \sim 2100(B/2)^{1/2} + O(1)$	$Re_c \sim 1050(B/2)^{1/2} + O(1)$
Hedström [18]	Compute numerically	Compute numerically
Mishra and Tripathi [23]	$Re_c \sim 525B + O(B^{1/2})$	$Re_c \sim 405B + O(B^{1/2})$
Slatter [24]	$Re_c \sim 590.63B + O(B^{1/2})$	$Re_c \sim 590.63B + O(B^{1/2})$

2. In Mishra and Tripathi’s expressions, the parameter C is a function of B , defined for the pipe by

$$C = \int_0^1 W^3(r)r \, dr = \frac{B^3(1 - r^*)^6}{8r^*} \left[\frac{1}{2} + \frac{1 - r^*}{(r^*)^2} \left(\frac{1 - r^*}{8} + \frac{16r^*}{35} \right) \right]. \tag{75}$$

For the plane channel, we have extended the criterion and C is defined by

$$C = \int_0^1 W^3(y) \, dy = \frac{B^3(1 - y^*)^6}{8y^*} \left[1 + \frac{16}{35} \frac{1 - y^*}{y^*} \right]. \tag{76}$$

3. In Slatter’s criterion, D_{ann} is a dimensionless hydraulic diameter of the yielded annulus and analogously, $D_s = 4(1 - y^*)$. The dimensionless parameters W_{ann} and W_s are defined by

$$W_{\text{ann}} = \frac{2}{1 - (r^*)^2} \int_{r^*}^1 W(r)r \, dr = \frac{B(1 - r^*)^2}{r^*(1 + r^*)} \left[\frac{2}{3}r^* + \frac{1 - r^*}{4} \right], \tag{77}$$

$$W_s = \frac{1}{1 - y^*} \int_{y^*}^1 W(y) \, dy = \frac{B(1 - y^*)^2}{3y^*}. \tag{78}$$

4.5.1. Asymptotic behaviour

Asymptotic values for all of these expressions can be derived in the two limits $B \rightarrow 0$ and $B \rightarrow \infty$. The behaviour of r^* and y^* in these limits is described in (13)–(15). In the limit $B \rightarrow 0$, we recover the Newtonian values for the critical Reynolds number in any of the above expressions. The limiting expressions for the critical Reynolds numbers, $Re_c(B)$ as $B \rightarrow \infty$, are given in Table 2.

Notes.

1. In the limit $B \rightarrow \infty$, the limiting value of Mishra and Tripathi’s parameter C in the pipe is

$$C \sim \frac{1}{2} + O(B^{-1/2}) \tag{79}$$

and in the plane channel is

$$C \sim 1 + O(B^{-1/2}). \tag{80}$$

2. In Slatter’s criterion, W_{ann} and W_s have the same limiting behaviour:

$$W_{\text{ann}} \sim \frac{2}{3} + O(B^{-1/2}) \quad \text{and} \quad W_s \sim \frac{2}{3} + O(B^{-1/2}). \tag{81}$$

5. Comparative results

Here, we provide a comparison of the different predictions made of transition. The results are slightly different in the case of the plane channel and the pipe, since in the case of the plane channel, we also have computed predictions of $Re_{lin}(B)$. Our comparison between theoretical and phenomenological criteria is not direct; the phenomenological criteria are *predictions* of a transitional Reynolds number, whereas our linear and nonlinear stability criteria are upper and lower bounds for transitional instabilities. As the nonlinear bound, we present $Re_{CB}(B)$ rather than $Re_{GB}(B)$. Our reasoning is that $Re_{CB}(B)$ is a conditional bound that indicates stability to perturbations that are of the same size as the mean flow. This is consistent with what one might expect in an experimental study of transition, i.e. transition typically occurs with a *small* finite perturbation.

In Fig. 3, we show the variations of the critical Reynolds number for transition, Re_c , as a function of a Bingham number B for the plane channel. Curve 7 in Fig. 3 shows $Re_{lin}(B)$, the lowest known value for which the flow is linearly unstable. Note that even if there exists a three-dimensional linear instability at lower Reynolds number than $Re_{lin}(B)$ (i.e. since Squire's theorem does not necessarily hold), $Re_{lin}(B)$ still provides an upper bound for transition, but perhaps not the least upper bound. Curve 6 in Fig.3 shows the conditional bound for nonlinear stability $Re_{CB}(B)$. Fig. 4 shows the same comparison for the pipe flow results.

A number of observations can be made.

1. All the criteria indicate an increase of Re_c with increasing B .
2. For all B , the phenomenological predictions $Re_c(B)$ are ranged in the same way for the two flows:

$$Re_{c,Hanks} < Re_{c,Metzner} < Re_{c,Mishra} < Re_{c,Slatter}. \quad (82)$$

For sufficiently large B , we also have that $Re_{c,Hedström} > Re_{c,Slatter}$.

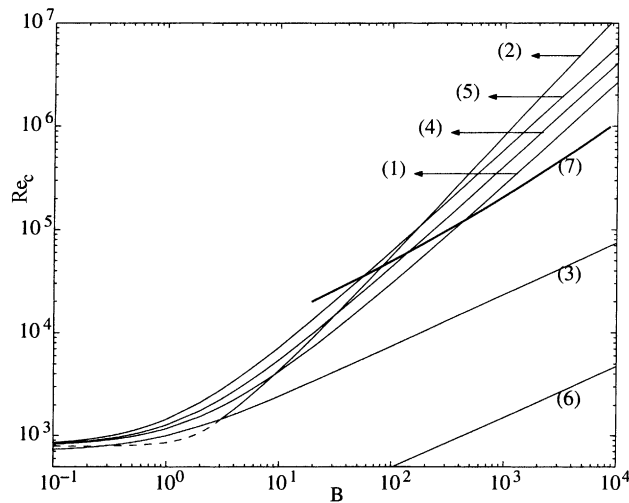


Fig. 3. Critical Reynolds number as a function of a Bingham number for plane channel flow: comparison between the different criteria —(1) Metzner and Reed criterion; (2) Hedström criterion; (3) Hanks criterion; (4) integral stability criterion; (5) Slatter criterion; (6) conditional stability; (7) linear stability.

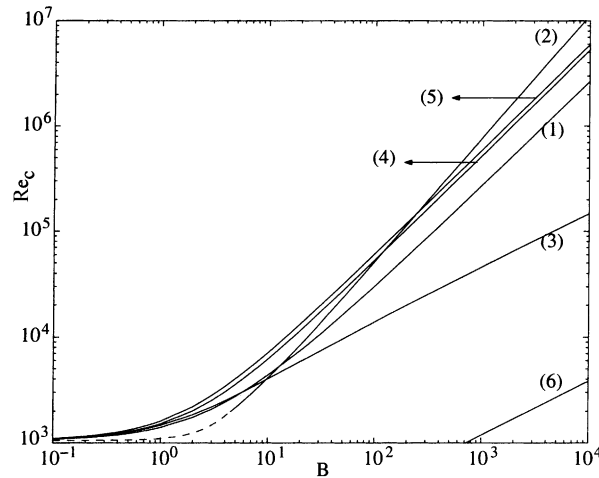


Fig. 4. Critical Reynolds number as a function of a Bingham number for pipe flow geometry: comparison between the different criteria—(1) Metzner and Reed criterion; (2) Hedström criterion; (3) Hanks criterion; (4) integral stability criterion; (5) Slatter criterion; (6) conditional stability.

3. For the plane channel, for $B > 200$, only Hanks criterion [20] lies between the two theoretical limits. If we consider the asymptotic behaviours in Table 2, it is observed that each of the other limits increases linearly with B and at a much greater rate than the linear stability bound. Unless there exists a value for B at which the transition ceases to be subcritical (thought to be very unlikely), each of these criteria must eventually fail to have any predictive validity.
4. In fact, for the plane channel flow, the asymptotic rate of increase of each of the phenomenological criteria is approximately one order of magnitude larger than the rate of increase of the linear stability bound $Re_{lin}(B)$. The asymptotic expressions in Table 2 actually approximate the full expressions for Re_c in Table 1 quite well, even for relatively low values of B , e.g. the approximation is reasonable at $B = 10$ and is very close after $B = 30$. Thus, the range in B over which any of the phenomenological criteria, apart from that of Hanks, is likely to accurately describe transition is actually fairly limited.

As we approach the limit $B \rightarrow 0$, the different phenomenological criteria are in agreement, since they are based on the same Newtonian value. A comparison of the different phenomenological criteria in the lower range of B is given in Fig. 5. The Hedström curve is based on the Nikuradse relation, which is valid for $Re_{Dh} \geq 4000$ (where Re_{Dh} is Reynolds number based on hydraulic diameter). Thus, to construct Fig. 5 this curve has been extrapolated to the Newtonian value, as indicated by the dashed line. It should be noted that the critical Reynolds number based on the intersection method assumes that the abrupt jump in frictional pressure loss (characteristic of Newtonian flow) is absent. In addition, the success of this method depends on the accuracy of the turbulent correlation used. In comparison with the other criteria (leaving Hanks criterion aside), Figs. 3–5 indicate that the Newtonian model (Nikuradse relation) tends to underestimate Re_c for low values of B , and overestimate Re_c for large B . Finally, the immediate observation from Fig. 5 is that even relatively close to $B = 0$, the different phenomenological criteria diverge significantly.

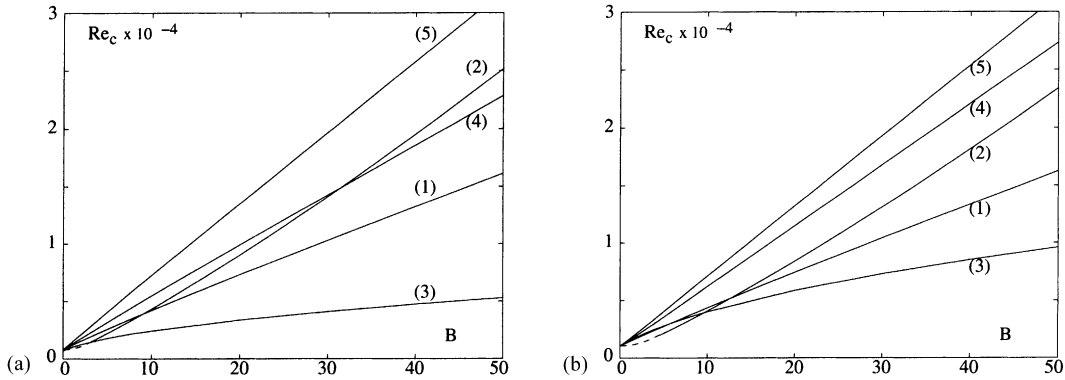


Fig. 5. Comparison between the different phenomenological criteria: (a) plane channel flow, (b) pipe flow—(1) Metzner and Reed criterion; (2) Hedström criterion; (3) Hanks criterion; (4) integral stability criterion; (5) Slatter criterion.

6. Discussion

The main contribution of the paper has been to derive new bounds for nonlinear stability of Poiseuille flow of a Bingham fluid. Both bounds $Re_{GB}(B)$ and $Re_{CB}(B)$ increase like $B^{1/2}$ as $B \rightarrow \infty$. The bound $Re_{GB}(B)$, although extremely weak, provides the first rigorous demonstration that this rate of increase is minimal and indeed that a Bingham fluid Poiseuille flow is more stable than its Newtonian ($B = 0$) counterpart, i.e. for sufficiently large B .

It is therefore gratifying to observe that no phenomenological prediction shows a rate of increase less than $B^{1/2}$ as $B \rightarrow \infty$. The fact that all criteria (and both linear and nonlinear bounds), increase with B is intuitively expected, but is not a priori an obvious result. Viscosity can play a dual role in the physical mechanism of transition. On the one hand, viscosity dissipates energy and the same dissipative role allows dissipative transfer of energy from the basic flow to the perturbation.

Exactly why Hanks criterion [20] gives lower values of Re_c is not entirely clear, except algebraically. The only real difference is that Hanks (and Ryan and Johnson) define their criteria by examining a ratio that varies locally across the basic flow, whereas the other criteria are based on global quantities derived from the mean flow.

Our results demonstrate conclusively that, for the plane channel, all phenomenological criteria except that of Hanks (equivalently Ryan and Johnson) become invalid at large B , since the linear stability bound is violated. Considering the pipe flow, we do not expect that the actual rate of increase of Re_c with B will differ by an order of magnitude from the results in the plane channel, nor do we expect that the asymptotic rate of increase should be different. Therefore, we strongly expect that all the rates of increase that are asymptotically linear with B in Table 2 (i.e. all except that of Hanks), are also invalid in the limit $B \rightarrow \infty$ for the pipe flow. These criteria simply increase too fast with B . The asymptotic rates of increase are approached rapidly for $B \geq 10$ in both geometries (see Fig. 5). In contrast, our results do not indicate whether Hanks criterion, or any of the others, gives a good prediction. All criteria are equally valid within the most practical range of B , say $B \in [0, 50]$, in the sense that neither theoretical limit is violated. A significant difference between the criteria is shown in Fig. 5, and the only way to determine which of the criteria is most applicable would be to compare with experimentally derived values.

Most of experimental studies of transition for yield stress fluids are based on frictional pressure loss measurements. As an example, a recent attempt to empirically characterise transition in large pipes has been made by Slatter and Wasp [25]. In [25], three correlations are presented, to cover transitional Reynolds numbers over the full range of Hedström number. Translated into our parameters, Re and B , these correlations and ranges are approximately:

$$Re_c \approx \begin{cases} 1050B, & B \leq 0.4047, \\ 1701.39B^{0.538}, & 0.4047 < B < 27.126, \\ 676B, & 27.126 \leq B. \end{cases} \quad (83)$$

Whilst the mid-range correlation is close to $B^{1/2}$, the high range correlation is similar to those in Table 2. The data set extends only up to $B \approx 100$ and is in fact based on fluids that are first characterised as Herschel–Bulkley fluids and then the rheological behaviour is somehow extrapolated to the Bingham fluid model.

Studies such as by Slatter and Wasp [25] highlight two key problems with studying transition experimentally for a Bingham fluid. Firstly, few fluids that have a yield stress show a completely linear relationship between $\hat{\tau}$ and $\hat{\gamma}$ over a sufficiently wide range of to make the Bingham fluid characterisation reasonable for a study of transition. However, for theoretical work, Bingham fluids are easier analytically and are the natural starting point for understanding what a yield stress does to a flow. Secondly, the method used to identify transition in an industrial flow is often based on detecting the change in frictional pressure drop. For several non-Newtonian fluids (especially slurries), the abrupt change in frictional pressure loss at transition is largely absent (see, for example [26,27]). Thus, some caution is needed in interpreting transition data for industrial slurry flows, e.g. are we seeing the start or finish of transition? A number of secondary local measurements should be made for comparison. We have found only three papers [26,28,29] dealing in detail with the flow properties near the transition. The centreline velocity is measured with help of LDV system [26,28]. Detection of transition is based on the fact that for laminar pipe flow the centreline velocity is substantially larger than for turbulent flow. Ideally, the time trace of the axial velocity at different radial locations should be analysed, in order to detect the first appearance of the turbulence burst corresponding to the start of transition. This kind of analysis has not, to our knowledge, been done for the fluids with which we are concerned. As a final comment concerning experimental studies for visco-plastic flows, we note that there have been many experimental correlations and phenomenological expressions for the frictional pressure losses in turbulent flows of industrial suspensions and slurries. Our results have no direct bearing on these results, except in questioning the prediction of the point at which transition occurs for large B .

As a theoretical problem, questions of transition and flow instability are perfectly well defined, if difficult. Both the nonlinear bounds here and the linear stability bounds in [1] give little deep insight into the actual instability mechanisms. We close with a few pertinent remarks.

Remarks.

1. If we examine the energy equations, either (17) or (18), we see that the inertial term takes its contribution only from the yielded region of the basic flow, regardless of size of perturbation, i.e. energy is transferred only in regions where the basic flow has a velocity gradient. The dissipation term may have contributions from the unyielded region of the basic flow, but these contributions have been shown to be negative and act to stabilise the flow. In this precise sense only, flow instability may be thought to

depend only on the characteristics of the unyielded flow region.

2. We note that in [1], the linear stability problem was determined via an eigenvalue problem that was defined only on the yielded region of flow.
3. With regard to observations (1) and (2) above, it is tempting to ignore the unyielded flow region in studying flow instability. However, this region is not a neutrally buoyant *solid* body immersed in the flow, nor is the yielded flow equivalent to a Newtonian fluid flow in an annulus with the inner cylinder translated axially at the plug velocity. Thus, ignoring the unyielded region is not thought sensible for theoretical study.
4. It is interesting to observe in Section 3.2 that our treatment of the dissipative terms results in only purely *viscous* dissipation, i.e. the terms involving B in the constitutive relations do not appear in (27); there is no direct *plastic* contribution to the dissipation. The only way in which B enters our bounds later is by the effect on the width of yielded fluid and via the velocity gradient of the basic flow, appearing in the inertial term. In a stable regime, where our nonlinear bounds are satisfied, we will achieve a monotonic (exponential) decay of our initial perturbation. It would be interesting to find and study special perturbations of our mean flow that allow a direct contribution of the plastic dissipation terms to an energy bound. For such perturbations, we might expect estimates for the decay of $H(t)$ that are faster than exponential.
5. As a purely mathematical exercise, we could attempt to improve our stability bounds via numerical solution of the eigenvalue problems arising in Section 3.4.
6. If we allow that the Bingham model is an idealisation of reality, there are usually two different approaches to modelling behaviour below the yield stress limit. First, we could assume that the fluid has in fact no yield stress and investigate the stability problem for a *regularised* version of the Bingham model, as is often done for steady flow computations. Second, we could assume that the yield stress limit in fact corresponds to a regime in which the material behaves as an elastic solid (as in Oldroyd's early formulation [30]). Both cases lead to interesting stability problems to be studied.

References

- [1] I.A. Frigaard, S.D. Howison, I.J. Sobey, On the stability of Poiseuille flow of a Bingham fluid, *J. Fluid Mech.* 263 (1994) 133–150.
- [2] H. Salwen, C. Grosch, The stability of Poiseuille flow in a pipe of circular cross-section, *J. Fluid Mech.* 54 (Part 1) (1972) 93–112.
- [3] A. Davey, P.G. Drazin, The stability of Poiseuille flow in a pipe, *J. Fluid Mech.* 36 (Part 2) (1969) 209–218.
- [4] V.K. Garg, W.T. Rouleau, Linear stability of pipe Poiseuille flow, *J. Fluid Mech.* 54 (Part 1) (1972) 113–127.
- [5] N. Itoh, Nonlinear stability of parallel flows with subcritical Reynolds numbers. Part 2. Stability of pipe Poiseuille to finite axisymmetric disturbances, *J. Fluid Mech.* 82 (Part 3) (1972) 469–479.
- [6] F.H. Busse, Bounds on the transport of mass and momentum by turbulent flow between parallel plates, *Z. Angew. Math. Phys.* 20 (1969) 1–14.
- [7] D.D. Joseph, S. Carmi, Stability of Poiseuille flow in pipes, annuli, and channels, *Quart. Appl. Math.* 26 (1969) 575–599.
- [8] D.D. Joseph, *Stability of Fluid Motions*, Vol. I, Springer, Berlin, 1976.
- [9] G. Duvaut, J.L. Lions, *Inequalities in Mechanics and Physics*, Springer, Berlin, 1976 (Chapter 6).
- [10] J.U. Kim, On the initial-boundary value problem for a Bingham fluid in a three-dimensional domain, *Trans. Am. Math. Soc.* 304 (2) (1987) 751–770.
- [11] J.U. Kim, On the Cauchy problem associated with the motion of a Bingham fluid in the plane, *Trans. Am. Math. Soc.* 298 (1) (1986) 371–400.

- [12] A.B. Metzner, J.C. Reed, Flow of non-Newtonian fluids — correlation of the laminar, transition and turbulent-flow regions, *AIChE J.* 1 (1955) 434–440.
- [13] O.C. Jones, An improvement in the calculation of turbulent friction in rectangular ducts, *ASME J. Fluids Eng.* 96 (1976) 173–181.
- [14] O.C. Jones, An improvement in the calculation of turbulent friction in smooth concentric annuli, *ASME J. Fluids Eng.* 103 (1981) 615–623.
- [15] W. Kozicki, C. Chou, C. Tiou, Non-Newtonian flow in ducts of arbitrary cross-sectional shape, *Chem. Eng. Sci.* 21 (1966) 665–679.
- [16] M. Sourlier, Contribution à l'étude des propriétés convectives de fluides thermodépendants. Cas de l'écoulement en canal de section rectangulaire. Ph.D. Thesis, Université de Nancy I, 1988.
- [17] M. Kostic, J.P. Hartnett, Predicting turbulent friction factors of non Newtonian fluids in non circular ducts, *Int. Comm. Heat Mass Transfer* 11 (1984) 345–352.
- [18] B.O.A. Hedström, Flow of plastic materials in pipes, *Ind. Eng. Chem.* 44 (3) (1952) 652–656.
- [19] N.W. Ryan, M.M. Johnson, Transition from laminar to turbulent flow in pipes, *AIChE J.* 5 (1959) 433–435.
- [20] R.W. Hanks, The laminar–turbulent transition for fluids with a yield stress, *AIChE J.* 9 (1963) 306–309.
- [21] R.W. Hanks, D.R. Pratt, On the Flow of Bingham Plastic Slurries in Pipes and Between Parallel Plates, Society of Petroleum Engineers Paper No. SPE 1682, 1967.
- [22] R.W. Hanks, A theory of laminar flow stability, *AIChE J.* 15 (1) (1963) 25–28.
- [23] P. Mishra, G. Tripathi, Transition from laminar to turbulent flow of purely viscous non-Newtonian fluids in tubes, *Chem. Eng. Sci.* 26 (1971) 915–921.
- [24] P.T. Slatter, The laminar–turbulent transition prediction for non-Newtonian slurries, in: *Proceedings of the International Conference on Problems in Fluid Mechanics and Hydrology*, Vol. 1, Prague, 1999, pp. 247–256.
- [25] P.T. Slatter, E.J. Wasp, The laminar–turbulent transition in large pipes, in: *Proceedings of the 10th International Conference on Transport and Sedimentation of Solid Particles*, Wroclaw, Poland, 4–7 September 2000.
- [26] J.T. Park, R.J. Mannheimer, T.A. Grimley, T.B. Morrow, Pipe flow measurements of a transparent non-Newtonian slurry, *ASME J. Fluids Eng.* 111 (1989) 331–336.
- [27] R.M. Turian, T.W. Ma, F.L.G. Hsu, D.J. Sung, Flow of concentrated non-Newtonian slurries. 1. Friction losses in laminar, turbulent and transition flow through straight pipe, *Int. J. Multiphase Flow* 24 (2) (1998) 225–242.
- [28] M.A. Abbas, C.T. Crowe, Experimental study of the flow properties of a homogeneous slurry near transitional Reynolds numbers, *Int. J. Multiphase Flow* 13 (3) (1987) 357–364.
- [29] M.P. Escudier, F. Presti, Pipe flow of a thixotropic liquid, *J. Non-Newtonian Fluid Mech.* 62 (1996) 291–306.
- [30] J.G. Oldroyd, A rational formulation of the equations of plastic flow for a Bingham solid, *Pror. Camb. Philos. Soc.* 43 (1947) 100–105.